The Astrophysical Journal, 781:99 (8pp), 2014 February 1 doi:10.1088/0004-637X/781/2/99

NORTH–SOUTH ASYMMETRIC SOLAR CYCLE EVOLUTION: SIGNATURES IN THE PHOTOSPHERE AND CONSEQUENCES IN THE CORONA

I. I. Virtanen and K. Mursula
University of Oulu, P. O. Box 3000, FI-90014 Oulu, Finland; ilpo.virtanen@oulu.fi
Received 2013 June 28; accepted 2013 December 1; published 2014 January 14

ABSTRACT

The heliospheric current sheet is the continuum of the coronal magnetic equator that divides the heliospheric magnetic field into two sectors (polarities). Several recent studies have shown that the heliospheric current sheet is southward shifted during approximately 3 years in the solar declining phase (the so-called bashful ballerina phenomenon). In this article we study the hemispherical asymmetry in the photospheric and coronal magnetic fields using Wilcox Solar Observatory measurements of the photospheric magnetic field since 1976 as well as the potential field source surface model. Multipole analysis of the photospheric magnetic field shows that during the late declining phase of solar cycles since the 1970s, the "bashful ballerina phenomenon" is a consequence of the g_2^0 quadrupole term, signed oppositely to the dipole moment. Surges of new flux transport magnetic field from low latitudes to the poles, thus leading to a systematically varying contribution to the g_2^0-term from different latitudes. In the case of a north–south asymmetric flux production, this is seen as a quadrupole contribution traveling toward higher latitudes. When the quadrupole term is largest, the main contribution comes from the polar latitudes. At least during the four recent solar cycles, the g_2^0-term arises because the magnitude of the southern polar field is larger than the magnitude found in the north in the declining phase of the cycle. In the heliosphere this hemispheric asymmetry of the coronal fields is seen as a southward shift of the heliospheric current sheet by about 2°.

Key words: Sun: corona – Sun: heliosphere – Sun: photosphere

Online-only material: color figures

1. INTRODUCTION

The first evidence of the momentary southward shift of the heliospheric current sheet (HCS) was found in the cosmic ray measurements of the *Ulysses* probe during the solar minimum of 1990s (Simpson et al. 1996). Reanalyzing heliospheric magnetic field (HMF) observations at 1 AU since the 1960s Mursula & Hiltula (2003) showed that the southward shift of the HCS has a systematic long-term occurrence in the late declining phase of the solar cycle, now called the "bashful ballerina." HMF sector polarities extracted from ground-based geomagnetic field observations proved that the HCS was shifted southward during cycles before space age, at least since solar cycle 16 (Hiltula & Mursula 2006).

We recently analyzed the HMF polar field measurements from the three fast-latitude scans of *Ulysses* and showed that before the solar minima in 1990s and 2000s the northern polar field was weaker by an amount that corresponded to the HCS shift of about 2° (Virtanen & Mursula 2010). The magnitude of the HCS shift was the same in solar cycles 22 and 23 even though the HMF intensity decreased by nearly 40% from the minimum of cycle 22 to the next minimum (Smith & Balogh 2008). However the measurements at the ecliptic plane depict the asymmetry less systematically in cycle 23 than in cycle 22 because the weaker polar fields in cycle 23 widen the HCS region and mask the asymmetry at low latitudes (Mursula & Virtanen 2011).

The same "bashful ballerina" pattern of the northern polarity field covering a larger area in the declining phase was found in the solar coronal magnetic field extrapolated from the photospheric magnetic field by the potential field source surface (PFSS) model (Zhao et al. 2005). Zhao et al. (2005) also found a strong quadrupole term oppositely oriented to the dipole term during times of HCS shift and showed that the quadrupole changed its polarity in phase with the leading dipole term from minimum to minimum. Accordingly, the HCS shift remains oriented in the same southward direction in every minimum (Zhao et al. 2005; Mursula & Hiltula 2004). Since the quadrupole term is hemispherically symmetric and the dipole term antisymmetric, their combination is hemispherically asymmetric. For example, during a positive solar minimum (positive dipole term) the positive polarity field dominates in the northern hemisphere and the negative polarity in the southern hemisphere. A simultaneous negative quadrupole term adds a negative polarity field to the high latitudes of both the northern and southern hemisphere. Combining the dipole and the quadrupole fields then leads to a smaller (larger) field magnitude in the northern (southern) polar region and a southward-shifted HCS. During a negative solar polarity minimum the quadrupole term is positive, leading to the same north–south asymmetry in field intensities and areas and, again, a southward-shifted HCS.

In a recent article Wang & Robbrecht (2011) suggested that the HMF polarity at the heliographic equator and the HCS shift are defined by prior north–south asymmetric sunspot activity. Using a flux transportation model they showed that the HCS was shifted southward or northward, depending on the polarity of the leading sunspot in the more active hemisphere. If the leading sunspot polarity in the more active hemisphere has the same (opposite) sign as the polar field in that hemisphere, the HCS is shifted toward the hemisphere with weaker (stronger) sunspot activity.

Momentary excess of sunspots in either hemisphere is a very common pattern, and there are also periods of more persistent differences between northern and southern hemisphere sunspot activity. Smoothed monthly sunspot numbers show that sunspot activity in the recent cycles has been larger during the ascending phase of solar cycle in the northern hemisphere and during the declining phase in the southern hemisphere (Vernova et al. 2002; Temmer et al. 2006). This pattern leads to the southward-shifted HCS in the model by Wang & Robbrecht (2011).

In this article we study the coronal magnetic fields obtained by using the photospheric magnetic field observed at the Wilcox Solar Observatory (WSO) and the PFSS model. We investigate the origin of the quadrupole moment in the photospheric magnetic field, its temporal evolution, and the formation of the north–south asymmetric coronal magnetic field. We discuss the hemispheric difference in polar field strengths and the evolution of the north–south asymmetry since 1970s. The article is organized as follows: Section 2 describes the WSO data and the numerical methods used in this work. In Sections 3, 4, and 5 we present the results for the HCS shift, the role of the quadrupole, and the north–south asymmetric flux transport. We discuss the results in Section 6. Section 7 presents our conclusions.

2. DATA AND METHOD

We use the photospheric magnetic field observed at the WSO since Carrington rotation 1642 in 1976. Measured values of the line-of-sight magnetic field are collected at WSO in rotational synoptic maps where the resolution in heliographic longitude is 5° (72 bins per rotation). In latitude there are 30 bins in equal steps of sine latitude from +14.5/15 to −14.5/15, corresponding to the highest latitude bin centered at ±75.°2. With sine latitude sampling each value in the synoptic map refers to a solar surface cell with roughly the same area.

The coronal field is calculated from the photospheric field using the PFSS model (Altschuler & Newkirk 1969; Schatten et al. 1969; Hoeksema et al. 1983). The PFSS model is based on the assumption that the region inside the source surface (SS: here we use a 2.5 solar radii) is current-free, and the field is purely radial at the SS, which gives the outer boundary condition. The inner boundary condition is formed by using the measured photospheric magnetic field under the assumption that the field is radial. With this condition the line-of-sight component at the central meridian divided by the cosine of the latitude gives the local (total) radial magnetic field. The current-free condition leads to a Laplace equation whose solution can be expressed in terms of harmonic coefficients g_n^m and h_n^m. This method is described in detail in WSO documentation (Wilcox Solar Observatory 2009). The radial component of the magnetic field between photosphere and SS is

$$B_r(r,\theta,\phi) = \sum_{n=1}^{9}\sum_{m=0}^{n} P_n^m(\cos\theta)\left(g_n^m \cos m\phi + h_n^m \sin m\phi\right) \times C(r,n), \quad (1)$$

where $P_n^m(\cos\theta)$ are the associated Legendre functions and r is the radial distance.

The radial functions $C(r,n)$ are

$$C(r,n) = \left(\frac{R}{r}\right)^{n+2}\left[\frac{n+1+n\left(\frac{r}{r_{ss}}\right)^{2n+1}}{n+1+n\left(\frac{R}{r_{ss}}\right)^{2n+1}}\right], \quad (2)$$

where R is the solar radius and r_{ss} is the SS radius (2.5 R).

Harmonic coefficients g_n^m and h_n^m are as follows:

$$\begin{Bmatrix} g_n^m \\ h_n^m \end{Bmatrix} = \frac{2n+1}{30\cdot 72}\sum_{i=1}^{30}\sum_{j=1}^{72}\frac{B_{j,i}^{\rm phot}}{\sin\theta_i} P_n^m(\cos\theta_i)\begin{Bmatrix}\cos(m\phi_j)\\ \sin(m\phi_j)\end{Bmatrix}, \quad (3)$$

where $B_{j,i}^{\rm phot}$ refers to the measured photospheric line-of-sight value at longitude–latitude bin (j,i), and $\sin(\theta_i)^{-1}$ term comes from the assumption of the radial magnetic field in the photosphere. The denominator $30\cdot 72$ counts the number of surface elements in the synoptic map.

After calculating the coronal magnetic field at the SS we sum up all bins of each magnetic polarity to find the total solid angles Ω_{ss}^+ (Ω_{ss}^-) covered by the positive (B_r away from the Sun) and negative (B_r toward the Sun) polarity.

Making the simplifying assumption of longitudinal symmetry (flat HCS), we can integrate the solid angle covered by the positive polarity as follows:

$$\Omega_{ss}^+ = \int_0^{2\pi}\int_0^{\theta_m} \sin\theta d\theta d\phi = 2\pi(1-\cos\theta_m), \quad (4)$$

where θ_m is the polar angle (colatitude) between the positive magnetic pole and the magnetic equator. Solving for magnetic latitude $\lambda_m = (\pi/2) - \theta_m$ we get

$$\lambda_m = \arcsin\left(1 - \frac{\Omega_{ss}^+}{2\pi}\right), \quad (5)$$

which gives the (longitudinally averaged) shift (displacement) of the HCS from the Sun's magnetic dipole equator, i.e., the expected average location of the HCS, in terms of the solid angle covered by the positive polarity (Zhao et al. 2005). If λ_m systematically deviates from zero during several rotations, it depicts a larger area covered by either polarity.

The magnetic dipole equator and the heliographic equator are not aligned in general. The tilt angle α between the solar rotation axis and the magnetic dipole axis reaches its minimum during solar minimum and maximum during solar maximum. Following Zhao et al. (2005) we define the longitudinally averaged shift of the HCS from the heliographic equator as follows:

$$\lambda_h = \lambda_m \cos\alpha. \quad (6)$$

There are several methods to calculate α. We use the one defined by WSO, where α is the average of the maximum northern and southern extension of the HCS in each rotation. Here we study both λ_m and λ_h, as they include different information about HMF. The magnetic shift λ_m reveals the overall asymmetric nature of the HMF, showing directly whether one polarity dominates over the other. However λ_h describes the HCS shift from the heliographic equator, which is an important quantity especially when comparing the longitudinally averaged model results with observations in the heliosphere. Note also that during solar maximum times the HCS is far from flat, and there are even multiple current sheets. Therefore the longitudinally averaged shift is not a realistic assumption during solar maximum times.

The lower multipole terms, in particular the dipole terms g_1^0 and h_1^0, are the most significant for the HMF during most of the solar cycle. The lowest term leading to north–south asymmetry in the longitudinally averaged magnetic area and intensity is the quadrupole term g_2^0. A simple method to investigate the role of this term to the HCS shift is to remove it from the multipole expansion (1) and to recalculate the related shifts. Comparing the results from original and the modified expansion shows how much this term contributes to the asymmetry.

The quadrupole term g_2^0 is obtained from Equation (3) in the following form:

$$g_2^0 = \frac{5}{30\cdot 72}\sum_{i=1}^{30}\sum_{j=1}^{72}\frac{B_{j,i}^{\rm phot}}{\sin\theta_i}\frac{1}{2}(3\cos^2\theta_i - 1). \quad (7)$$

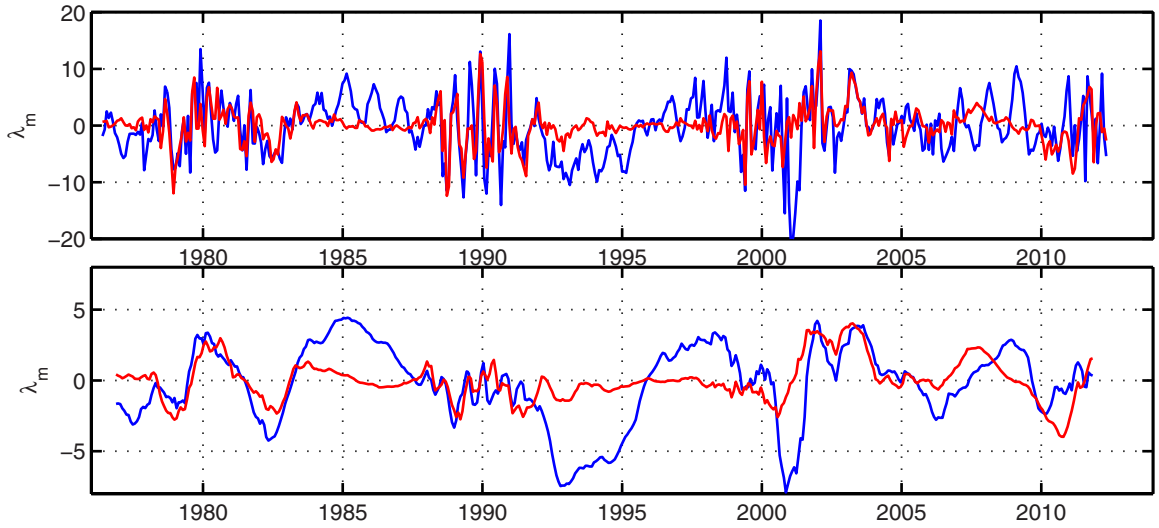

Figure 1. Longitudinally averaged HCS shift from the magnetic equator according to full expansion (full-field λ_m, blue) and to an expansion (nonquadrupole λ_m) where g_2^0 is neglected (red); values for each rotation (upper panel) and 13 rotation running means (lower panel).
(A color version of this figure is available in the online journal.)

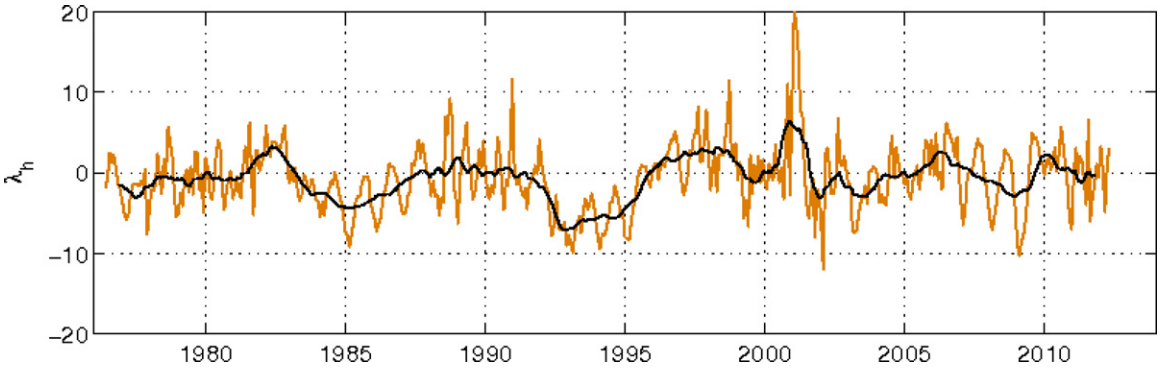

Figure 2. Longitudinally averaged HCS shift from the heliographic equator according to the full-field expansion, values for each rotation (orange line) and 13 rotation running mean (black line).
(A color version of this figure is available in the online journal.)

Since g_2^0 is axisymmetric it can be expressed as follows:

$$g_2^0 = \frac{5}{30 \cdot 2} \sum_{i=1}^{30} \frac{3\cos^2\theta_i - 1}{\sin\theta_i} \langle B_i^{\rm phot} \rangle, \quad (8)$$

where $\langle B_i^{\rm phot} \rangle$ refers to the longitudinal average of the measured line-of-sight magnetic field at latitude θ_i. Since g_2^0 is also hemispherically symmetric, it vanishes if the longitudinally averaged photospheric field is hemispherically antisymmetric, e.g., dipolar field.

3. HCS SHIFT DUE TO THE QUADRUPOLE MOMENT

Figure 1 shows λ_m, the longitudinally averaged shift of the HCS from the magnetic equator. The blue line refers to λ_m (hereafter called the full-field λ_m) calculated from the coronal PFSS model using the full expansion given in Equations (1)–(5). The red line depicts λ_m (hereafter called the nonquadrupole λ_m), where the quadrupole term g_2^0 has been neglected in the expansion of Equation (1).

Figure 2 shows the longitudinally averaged HCS shift from the heliographic equator λ_h according to full-field expansion. Orange line depicts the values for each rotation and black line 13 rotation running mean. Magnetic polarity (dipole axis) reverses from one cycle to another, whereas during positive solar minima such as those in the 1970s and 1990 λ_m and λ_h are oriented in the same direction, but in the negative minima of the 1980s and 2000s they are oriented oppositely. A comparison of Figures 1 and 2 shows that during solar minimum times when the tilt angle between the dipole axis and the solar rotation axis is small λ_m and λ_h are roughly equally large (but oppositely oriented during negative polarity times). During maximum times when the tilt angle is larger, λ_m values tend to have large momentary values, but λ_h fluctuates around zero.

Figure 1 shows that at the beginning of the data in 1976 both λ_m's follow the magnetic equator, but late in 1976 the full-field λ_m indicates a period of HCS shift toward the southern magnetic hemisphere, while the nonquadrupole λ_m remained at the equator. The southward shift of the full-field λ_m continued until 1978, which is in a very good agreement with a recent multispacecraft analysis using *Pioneer 10*, *Pioneer 11*, and OMNI data (Mursula & Virtanen 2012). At the solar maximum time around 1980 both full-field and nonquadrupole λ_m's oscillated strongly from one rotation to another, and there was neither a systematic HCS shift nor a systematic difference between the two λ_m's.

In the late declining phase of cycle 21 and around the next solar minimum from 1984 to 1987, the full-field HCS was again strongly shifted toward the southern magnetic hemisphere, but the shift did not exist in the nonquadrupole λ_m. Note that during this negative polarity minimum the shift toward the magnetic south is seen as an upward deflection in Figure 1 but downward (southward in the heliographic system) in Figure 2. During this minimum the polar fields were strongest, and the HCS was found to be thinner than ever during the space age (Richardson & Paularena 1997). From 1988 to 1991 there is a strong half-year oscillation both in the full-field and nonquadrupole λ_m. On the other hand, this oscillation is severely damped in Figure 2. This is related to the maximum time configuration where the dipole tilt angle α is large, and nonaxisymmetric components dominate the multipole expansion. Note also that no persistent (>1 yr) shift is found in either λ_m at this time, as described in the lower panel of Figure 1.

The full-field λ_m is found to be southward shifted again during the declining phase of cycle 22. The systematic difference between the full-field λ_m and the nonquadrupole λ_m started in 1992 and lasted until mid-1995. The southward HCS shift was very strong during this time, with 13 rotation means reaching a value above 5° for several years. From 1994 to 1995 the *Ulysses* probe completed its first pole-to-pole fast scan. Using the magnetic field observations of *Ulysses* it was found that the HCS was shifted southward by 2° at this time (Virtanen & Mursula 2010; Erdös & Balogh 2010).

From 1996 to 1998 the full-field λ_m indicated a fairly systematic northward shift of HCS, while the nonquadrupole λ_m mainly followed the heliographic equator. The exceptional orientation is best seen in Figure 2. We note that such a systematic northward HCS shift in the full-field λ_m is not found in any other of the four ascending phases (cycles 21 to 24) that are covered in this study. There is also a large momentary northward shift of the full-field λ_m in 2001, and a small shift in the nonquadrupole λ_m slightly earlier.

Solar cycle 23 was peculiar in many ways, and several solar parameters reached uncommon values, especially during the late declining phase of the cycle. The polar fields were exceptionally weak (Smith & Balogh 2008; McComas et al. 2008), and the HCS region was wider than during the previous minima (Mursula & Virtanen 2011), which led to a significant amount of both polarities on both sides of the ecliptic. In these conditions of the wide HCS region the sector occurrence ratios around the ecliptic do not necessary clearly depict the shift (Mursula & Virtanen 2011).

In Figure 1, the first HCS shifts toward the southern magnetic hemisphere in 2002 and 2003 are seen both in the full-field and nonquadrupole λ_m (and in λ_h in Figure 2). However, the shift development was halted in 2004, most likely due to the appearance of a persistent low-latitude coronal hole in the southern hemisphere that affected the HCS and streamer belt structure for several years (Mursula & Virtanen 2011). Accordingly, the HCS shift as studied by the WSO observations or by in situ HMF observations at 1 AU, remained smaller in solar cycle 23 than in earlier cycles (minima). (Even a weak northward shift was seen due to this development.) During its third fast-latitude scan in 2007, the *Ulysses* probe observed an asymmetry of the polar coronal fields, which corresponds to the southward shift of the HCS region by about 2° (Virtanen & Mursula 2010; Erdös & Balogh 2010). Interestingly, this HCS shift value agrees with the shift observed during the first scan from 1994 to 1995, although the polar fields in cycle 23 were considerably weaker than in cycle 22. The average southward shift of the full-field λ_m from 2007 to 2009 was only about 1°, i.e., smaller than the 2° shift derived from *Ulysses* measurements in 2007 or the shifts in WSO observations in the previous minima. This is likely due to the fact that because of the exceptional width of the HCS region in the declining phase of cycle 23, the polar fields are underweighted in the WSO data and in the PFSS expansion, which led to unreliable results about the asymmetry. In 2010 λ_m starts to oscillate rapidly in a way that is typical for solar maximum times as a response to the increasing solar activity of the new solar cycle 24.

The lower panel of Figure 1 shows the 13 rotation (roughly 1 yr) averages of the full-field and nonquadrupole λ_m, where the annual vantage point oscillation and shorter variations are removed. The thick line in Figure 2 depicts the 13 rotation average of λ_h. The vantage point effect is an artifact that arises from the annual variation of the Earth's heliographic latitude. When the Earth is at a high heliographic latitude the polar field from the opposite solar hemisphere is underestimated, and the PFSS model produces an artificial HCS shift toward the Earth's current hemisphere. Early in the year, when the Earth is below the heliographic equator, the field of the southern hemisphere is intensified by the vantage point effect, leading to a larger southward HCS shift. This is clearly seen in the upper panel of Figure 1 in 1985 and 1995 for the two opposite polarity minima. On the other hand, in the fall when the earth is above the heliographic equator, the southward HCS shift is reduced close to zero. The annual (13 rotation) averaged HCS shift shows a persistent nonzero southward deflection during "bashful ballerina" times, although the WSO estimate of the shift seems to be slightly overestimated due to the vantage point effect when comparing to the shift value observed from *Ulysses*. Note also that when removing the g_2^0 term from the multipole expansion the vantage point oscillation is almost completely reduced.

4. ORIGIN OF THE QUADRUPOLE

Equation (8) shows that different latitudes contribute to the axisymmetric g_2^0 quadrupole by different weights. Contribution from one latitude bin may be relatively large, but in most cases the northern and southern contributions from the same absolute latitude are oppositely signed and cancel each other out. That is why we also investigate the combined contribution from the two latitude bands at the same absolute latitude in the north and south. If the longitudinally averaged photospheric magnetic field is hemispherically antisymmetric (such as in the dipolar case), g_2^0 from each latitude band pair vanishes. Moreover, the global g_2^0 may also vanish even if the contributions from different latitude pairs are nonzero but happen to cancel out each other.

Figure 3 shows the total g_2^0 and its contributions from three different heliographic latitude regions: the highest (northern and southern) latitude bins centered at 75°.2 corresponding to the latitude range from ±69° to ±90°, mid-latitudes |36°.9–69°|, and the low latitudes around the equator from −36°.9 to +36°.9.

At the beginning of the data from 1976 to 1978 the quadrupole term mainly arises from the highest latitude region |69°–90°|. Around the maximum of cycle 21 other latitudes also attain large quadrupole terms. The polar fields dominate in the g_2^0-term again from 1985 to 1987 when the full-field λ_m and λ_h shifted. Before this time from 1983 to 1984, the low and midlatitudes gave a large contribution to the g_2^0-term, being thus largely responsible for the first part of the time interval of the southward-shifted HCS. This evolution suggest that the positive g_2^0-term

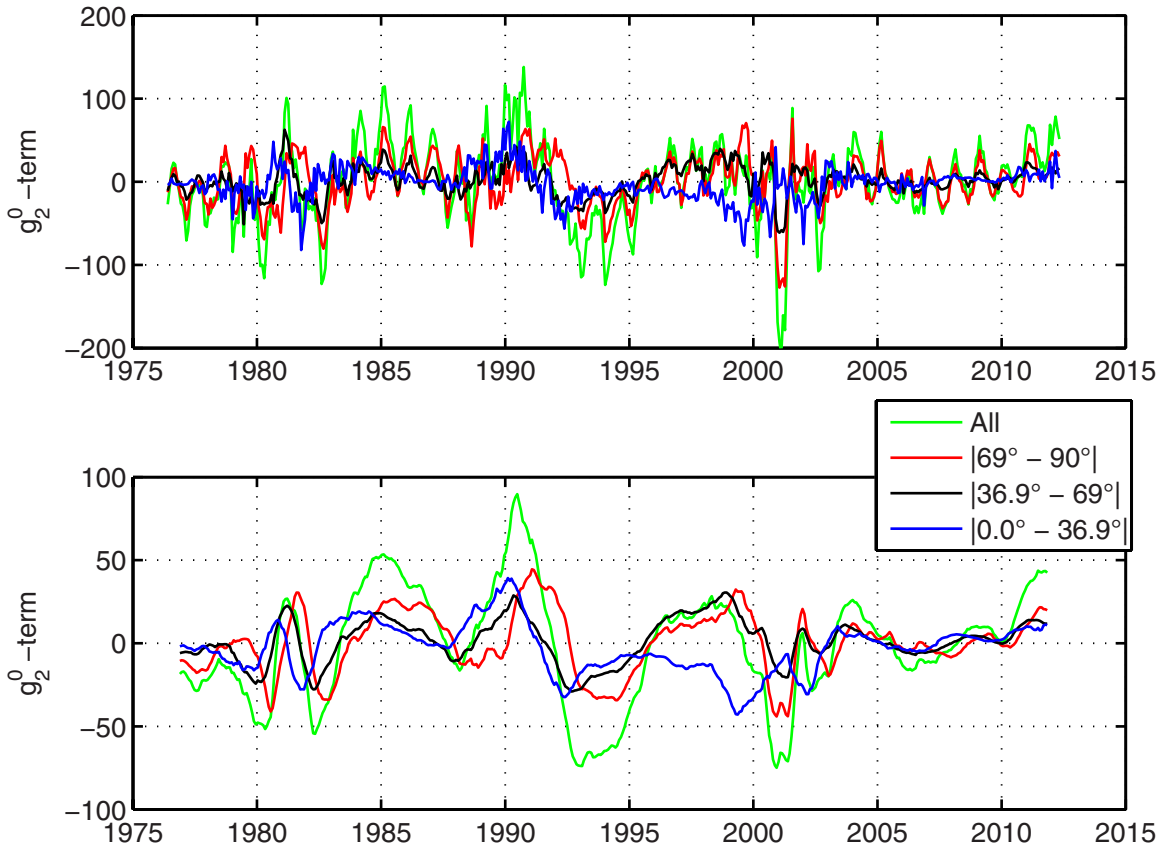

Figure 3. Quadrupole term g_2^0 (green) and its contributions from three latitude ranges; values for each rotation (upper panel) and 13 rotation running means (lower panel).

responsible for the HCS shift in mid-1980s first appeared at low latitudes and then moved to the poles remaining there longer than at other latitudes.

From 1988 to 1991 the g_2^0-term contribution from low latitudes was consistently positive, reaching a maximum in early 1990 followed by similar maxima in mid- and high-latitude contributions to g_2^0 (see Figure 3). As shown in Figure 1, λ_m (but not λ_h) depicted large semiannual oscillation at this time. Soon thereafter, the g_2^0-term turned negative for several years, repeating the pattern seen in the mid-1980s. Again, the (negative) g_2^0-term had its maximum first at low and mid-latitudes dissipating slowly to high latitudes, which again had the largest contribution to g_2^0-term during most of the "bashful ballerina" times from 1993 to 1996. As was seen in Figure 1, during the rising phase of cycle 23 from 1996 to 1998 the HCS is persistently shifted northward due to the positive g_2^0-term. Figure 3 shows that the low-latitude contribution to g_2^0 at this time is opposite to the contributions from the two other latitude ranges, leaving the total g_2^0 relatively weak. They roughly canceled each other out during the sunspot maximum from 1999 to 2000 when λ_m depicts rapid oscillations around zero due to higher multipoles. On the other hand the exceptionally large but fairly short northward shift of λ_h in 2001 (see Figure 2) attained a major contribution from the g_2^0-term, mainly from mid- and high latitudes. The northward expansion of the positive polarity from the south is very rapid and reached its maximum in 2001 January (the Carrington rotation of 1972) when positive polarity field covered 68% of the synoptic solar surface, which led to a momentary northward shift of λ_h by up to 21°.1 (see Figure 2). It is interesting to note that this exceptional evolution occurred at the time of the solar EUV/UV maximum of cycle 23, which started a period of exceptional magnetic evolution that has continues until the present time (Lukianova & Mursula 2011). A similar but weaker and slower expansion was seen in 2002. After 2005 the g_2^0-term was very small until the rising phase of cycle 24 in 2010.

The noise level was roughly the same in each original line-of-sight measurement, but with the assumption of the radial field at the photosphere the noise increases by a factor of four from equator to high latitudes as a consequence of the denominator $\sin\theta_i$ in Equation (7). The extremely weak polar fields during solar cycle 23 caused even a larger reduction of polar field signal-to-noise ratio. Accordingly, the measurements of the highest latitude fields that cause the largest contribution to the g_2^0-term and the southward shift of HCS in the mid-1980s and mid-1990s suffer badly from weaker polar fields in cycle 23 and the implied increase of the vantage point effect. (Note the very large amplitude of the annual variation of λ_m from 2007 to 2009.) This problem is already less severe in the second highest latitude bin of ±64°.2, where the vantage point effect is not so significant and whose contribution to the g_2^0-term is much smaller.

There are several methods that are being used to try to correct the magnetograph saturation (Svalgaard et al. 1978; Wang & Sheeley 1995) and to remove the annual oscillation (Sun et al. 2011). The methods used by Svalgaard et al. (1978) and Wang & Sheeley (1995) introduce correction factors, which are constant in time and hemispherically symmetric, thus only correcting the average magnitude of the field in order to find a better match with HMF measurements and leaving the vantage point effect unchanged. The correction by Sun et al. (2011) filters the polar

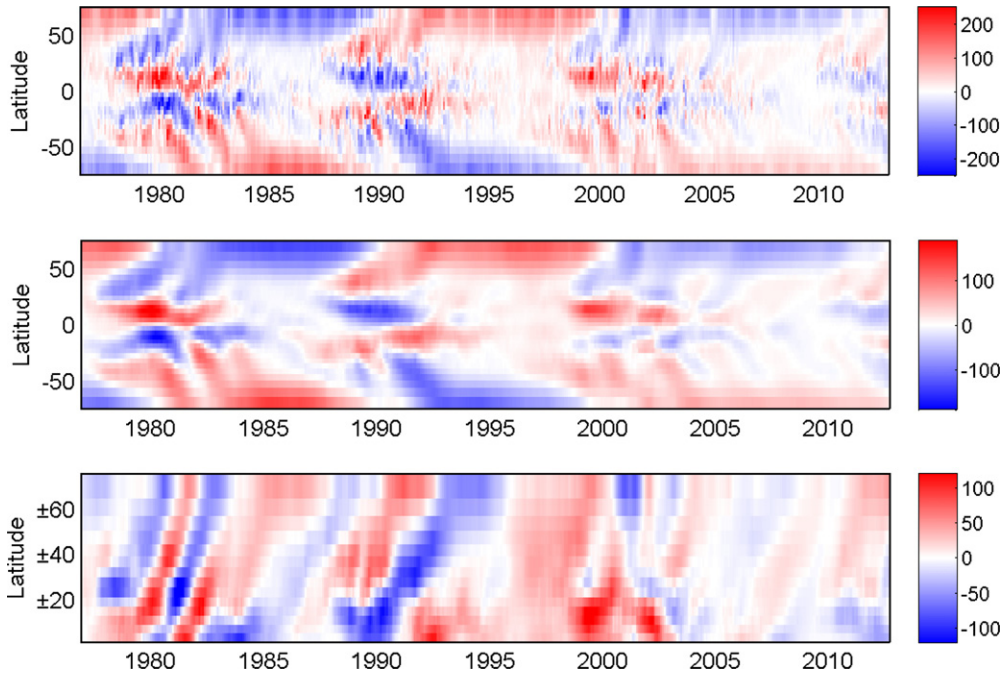

Figure 4. Magnetic butterfly diagram showing the longitudinally averaged line-of-sight photospheric magnetic field; one column for each rotation (top panel), 13 rotation running means (middle panel), north and south summed together and smoothed over 13 rotations (bottom panel).

field measurements using field values from lower latitudes and is able to remove the yearly oscillation in polar field magnitude. However, since the g_2^0-term attains its largest value from the highest latitude bins, correcting the polar fields by using even the second highest latitude bin would unavoidably underestimate the g_2^0-term. Because of these reasons we have not made any corrections to the Wilcox data used here.

5. NORTH–SOUTH ASYMMETRIC FLUX TRANSPORT

Figure 4 presents the butterfly diagram of the line-of-sight photospheric magnetic field measured at WSO. The upper panel of Figure 4 shows the longitudinally averaged photospheric magnetic field for each rotation, the middle panel shows the 13 rotation running means, and the bottom panel depicts the northern and southern field summed together and then averaged over 13 rotations. Figure 4 shows the poleward transport of flux that tends to occur in a series of discrete "surges" (Wang et al. 2009) or "ripples" (Ulrich & Tran 2013). These surges may include both polarities despite the ongoing reversal of the polar field. A simple estimate using the slope of the stripes in 1980s indicates a poleward flow velocity of about 10 m s^{-1} at midlatitudes, in an agreement with the results by Hathaway & Rightmire (2011).

At the beginning of the period investigated in 1976 the polar field in the north had a positive polarity and a negative polarity in the south. The first surges of opposite polarity toward poles start in 1977, beginning slightly earlier in the northern hemisphere. This surge reached the northern polar region in 1980 and reversed the northern polar field to negative. In Figure 3 this is seen as a negative quadrupole, which gains its contribution first from low latitudes and then from high latitudes. Figure 4 shows two surges of old positive polarity toward the north in 1980 and 1983. The first surge reversed the northern polarity to (weakly) positive for a short period in 1981, but the second surge did not reach latitudes higher than 40°. Both of these surges contributed to the positive quadrupole deflection (see Figure 3), although similar surges in the southern hemisphere have contributed more, especially since 1983.

The southern hemisphere behaves in a slightly different way. The first surge of new polarity also reached the southern polar region in 1980 and reversed the polarity there. However, the following surge of the old negative polarity reached the pole only in 1982.

A strong surge of positive polarity starting in 1982 made the final reversal of the southern pole in 1983, somewhat later than in the northern pole. Interestingly, an additional surge of new flux that started in 1983 gives additional strength to the southern polar field, and during the solar minimum time from 1984 to 1987 the southern polar field had a larger magnitude than the northern polar field. (A similar, roughly simultaneous surge of new polarity in the north remains considerable weaker.) The decay of the active regions and the related production of new flux had already ended in the north in 1983, but continued in the south until 1985. This development from 1983 to 1985, which led to the stronger field in the south and to the southward-shifted HCS, is also seen in Figure 3 in the development of a large positive quadrupole, which gains its main contribution first from low latitudes and then from high latitudes.

In cycle 22 the first surge of the positive polarity toward the north pole was observed to start in 1987, reaching the pole in 1990 and reversing the northern polar field permanently. The development of the southern polar field was again quite different from that in the north. Figure 4 shows that the first surge of negative polarity had already started in 1985, but proceeded very slowly and reversed the southern polar field momentarily. The strong surge of old positive polarity returned the positive polarity of the southern polar field in 1990. The simultaneous surges of positive polarity in both hemispheres in 1990 are clearly seen also in Figure 3 as a large positive g_2^0-term, whose contributions develop from low to high latitudes. Figure 4 shows that the final reversal of the southern polar field occurred in 1991, about one and a half years later than in the north. The surge, which reversed the polarity, was very strong and made

the southern polar field stronger from 1992 to 1995. In Figure 3 this is seen as a large negative g_2^0-term and in Figures 1–2 as a southward-shifted HCS.

As in cycle 21, the generation of new polarity flux started very early in the southern hemisphere in cycle 22. The first surge of positive polarity had already started in 1995 and reversed the southern pole in 1999. Interestingly, surges of old positive polarity were seen in the northern hemisphere until 1999, enhancing the intensity of the northern pole larger than in the south, which led to a positive quadrupole and an exceptional northward shifted HCS from 1996 to 1998.

The first surge in cycle 23 of the new polarity field in the north only started in 1998. This led to a rapid reversal of the northern field and, together with strong positive polarity field at low latitudes, to a very strong momentary negative g_2^0-term in 2000 (see Figure 3, an all-time minimum of λ_m (see Figure 1), and a strongly northward-shifted λ_h (see Figure 2).

The declining phase of solar cycle 23 differs from previous cycles in that there are several weak surges of both polarities in both hemispheres. Therefore polar fields did not gain much more strength after 2002 and remained weak over the whole minimum (Wang et al. 2009; Smith & Balogh 2008). The bottom panel of Figure 4 shows that the relative strength of the surges varies in time, with positive surges dominating in 2003, negative surges dominating in 2006, and positive surges again dominating from 2008 to 2009. These are seen as corresponding changes in the g_2^0-term (Figure 3), in λ_m (Figure 1), and in λ_h (Figure 2). Because of this inconstancy of the g_2^0-term, the southward shift of the HCS (λ_h) remains shorter and weaker than the shift observed in the two previous minima.

The production of the new polarity field in solar cycle 24 started more actively in the north in late 2009. The northern polar field reversed for the first time in 2011, but the old polarity returned after a few rotations. The southern polar field remained positive at least until the end of 2012. In Figure 3 this is seen as a positive g_2^0-term.

6. DISCUSSION

The results presented in this article verify that the systematic north–south asymmetry earlier observed in the heliospheric, coronal, and photospheric magnetic fields is a consequence of the different solar cycle evolution of magnetic fields in the northern and southern solar hemispheres. The ultimate internal cause of this hemispherical asymmetry is still partly unknown, but it clearly must be a permanent pattern of the solar dynamo, at least during the last several decades (Hiltula & Mursula 2006; Mursula & Hiltula 2004).

The butterfly diagram (Figure 4) shows that the transport of the magnetic flux of the decaying active regions toward the poles tends to occur in discrete surges of magnetic flux. Surges may have either magnetic polarity in any solar cycle phase, which is in an apparent contradiction with the Babcock–Leighton mechanism and Joy's law. The strength and the orientation of active regions (flux production), supergranular diffusion in the active region belt, and the meridional flow define the structure of surges and thereby the polar field strength.

A recent study suggests that the phase shift in the magnetic field evolution between the northern and southern hemispheres is a consequence of the north–south asymmetric meridional flow (McIntosh et al. 2013). Meridional flow plays an important role for the polar field magnitude and cycle length (Nandy et al. 2011), but determining the exact rate of the meridional flow is complicated (Hathaway 1996). There are at least three different methods to define the meridional flow speed: tracking the motion of magnetic elements (Hathaway & Rightmire 2010), investigation of the Doppler shift of the spectral lines (Ulrich 2010), and helioseismology (Gizon & Rempel 2008). Using the same method with different data sets gives fairly consistent results, but differences between results obtained using different methods are large (Ulrich 2010). For example, the results obtained by the Doppler shift method cannot explain variations in the polar field development, but meridional flow profiles obtained by magnetic feature tracking seem to be in agreement with measured polar field intensities (Janardhan et al. 2010). This indicates that the magnetic features move partly independently from the plasma flow.

Wang & Robbrecht (2011) performed flux transport simulations and suggested that the g_2^0-quadrupole and the related HCS shift could arise only from the north–south asymmetric strength of active regions, using a north–south symmetric meridional flow, differential rotation, and orientation of active regions. They also note that the flux generation is more active before the polarity reversal in the north and after the reversal in the south. If the new flux was distributed instantaneously, their model would imply that the HCS would be southward shifted both in the ascending and descending phase of the cycle. However we have found no significant southward shift of λ_h in the ascending phase. Instead the HCS was found to be northward shifted in the ascending phase of solar cycle 23.

The stronger flux generation of the northern hemisphere in the ascending phase probably causes the earlier reversal of the polar field in the northern hemisphere. So rather than causing the systematic shifts in HCS, the stronger activity in the north in the ascending phase contributes to the timing of the polar field reversal and the rise of the polar field asymmetry in the descending phase. The earlier reversal of the northern polar field may also contribute to its relative weakness later in the descending phase with respect to the southern polar field. This difference in field strength causes the southward HCS shift, and this remains a fairly stable pattern for several years in the late declining to minimum phase.

We have also seen that the appearance and transport of surges of new flux from low latitudes to high latitudes is a general pattern causing changes in the multipole pattern of the magnetic field and differences in polar field strength. This supports the model of Wang & Robbrecht (2011). Together with a hemispherically asymmetric generation of new flux, this contributes to the observed asymmetries. However we have also seen changes and differences in the meridional transport of these surges. In particular, it seems that the new flux appears earlier in the new cycle in the southern hemisphere and is transported to the pole more slowly.

7. CONCLUSIONS

In this article we have studied the hemispherical asymmetry in the photospheric and coronal magnetic fields. Multipole analysis of the photospheric magnetic field shows that during the late declining to minimum phase of solar cycles since the 1970s, there was a persistent g_2^0 quadrupole term that signed oppositely to the dipole moment and led to the southward shift of the HCS for about 3 yr in the late declining to minimum phase of solar cycle (the "bashful ballerina phenomenon"). On the other hand, in the ascending and maximum phase of the solar cycle, the higher order multipoles can, in addition to the quadrupole, significantly contribute to the HCS offset from the heliomagnetic equator, but these intervals remain typically

rather short and do not produce notable shifts with respect to the heliographic equator.

Surges of new flux transport magnetic field from the sunspot belt to the polar regions within a few years. Since flux production is north–south asymmetric, these surges produce significant but temporally limited contributions to the quadrupole g_2^0-term, which moves systematically from low to high latitudes. However the most persistent quadrupole term is obtained only when the asymmetry of the polar fields has been established in the late declining phase of the cycle, after the main flux transport has taken place. At least during the four recent solar cycles the g_2^0-term arises because the magnitude of the southern polar field during the declining phase of the cycle is larger than in the north, leading to the southward shift of the HCS.

The magnetic butterfly diagram shows that the solar cycle evolution of the photospheric magnetic field is hemispherically asymmetric. The northern hemisphere tends to be more active during the ascending phase of the cycle, which also seems to lead to an earlier polar field reversal in the northern hemisphere (Svalgaard & Kamide 2013). On the other hand, the larger flux generation in the southern hemisphere during the declining phase contributes to the stronger polar field in the south in the declining phase. In addition to the hemispheric asymmetry in the flux generation, the hemispheric asymmetry in the meridional flow seems to contribute to this asymmetry of polar fields and to the southward shift of the HCS in the late declining to minimum phase of the solar cycle.

We acknowledge the financial support by the Academy of Finland for HISSI project no. 128189. The research leading to these results has received funding from the European Commission's Seventh Framework Programs (FP7/2007–2013) under the grant agreements eHeroes (project 284461, http://www.eheroes.eu) and STORM (project 313038, http://www.storm-fp7.eu). Wilcox Solar Observatory data used in this study were obtained via the Web site http://wso.stanford.edu courtesy of J. T. Hoeksema.

REFERENCES

Altschuler, M. D., & Newkirk, G. 1969, SoPh, 9, 131
Erdös, G., & Balogh, A. 2010, JGRA, 115, 1105
Gizon, L., & Rempel, M. 2008, SoPh, 251, 241
Hathaway, D. H. 1996, ApJ, 460, 1027
Hathaway, D. H., & Rightmire, L. 2010, Sci, 327, 1350
Hathaway, D. H., & Rightmire, L. 2011, ApJ, 729, 80
Hiltula, T., & Mursula, K. 2006, GeoRL, 33, L03105
Hoeksema, J. T., Wilcox, J. M., & Scherrer, P. H. 1983, JGR, 88, 9910
Janardhan, P., Bisoi, S. K., & Gosain, S. 2010, SoPh, 267, 267
Lukianova, R., & Mursula, K. 2011, JASTP, 73, 235
McComas, D. J., Ebert, R. W., Elliott, H. A., et al. 2008, GeoRL, 35, 18103
McIntosh, S. W., Leamon, R. J., Gurman, J. B., et al. 2013, ApJ, 765, 146
Mursula, K., & Hiltula, T. 2003, GeoRL, 30, 2135
Mursula, K., & Hiltula, T. 2004, SoPh, 224, 133
Mursula, K., & Virtanen, I. I. 2011, A&A, 525, L12
Mursula, K., & Virtanen, I. I. 2012, JGRA, 117, 8104
Nandy, D., Muñoz-Jaramillo, A., & Martens, P. C. H. 2011, Natur, 471, 80
Richardson, J. D., & Paularena, K. I. 1997, GeoRL, 24, 1435
Schatten, K. H., Wilcox, J. M., & Ness, N. F. 1969, SoPh, 6, 442
Simpson, J. A., Zhang, M., & Bame, S. 1996, ApJL, 465, L69
Smith, E. J., & Balogh, A. 2008, GeoRL, 35, 22103
Sun, X., Liu, Y., Hoeksema, J. T., Hayashi, K., & Zhao, X. 2011, SoPh, 270, 9
Svalgaard, L., Duvall, T. L., Jr., & Scherrer, P. H. 1978, SoPh, 58, 225
Svalgaard, L., & Kamide, Y. 2013, ApJ, 763, 23
Temmer, M., Rybák, J., Bendík, P., et al. 2006, A&A, 447, 735
Ulrich, R. K. 2010, ApJ, 725, 658
Ulrich, R. K., & Tran, T. 2013, ApJ, 768, 189
Vernova, E. S., Mursula, K., Tyasto, M. I., & Baranov, D. G. 2002, SoPh, 205, 371
Virtanen, I. I., & Mursula, K. 2010, JGRA, 115, 9110
Wang, Y.-M., & Robbrecht, E. 2011, ApJ, 736, 136
Wang, Y.-M., Robbrecht, E., & Sheeley, N. R., Jr. 2009, ApJ, 707, 1372
Wang, Y.-M., & Sheeley, N. R., Jr. 1995, ApJL, 447, L143
Wilcox Solar Observatory 2009, PFSS Model Documentation, http://wso.stanford.edu/words/pfss.pdf
Zhao, X. P., Hoeksema, J. T., & Scherrer, P. H. 2005, JGRA, 110, 10101